Presynaptic homeostasis at CNS nerve terminals compensates for lack of a key Ca^{2+} entry pathway

Erika S. Piedras-Rentería*†‡, Jason L. Pyle*†, Max Diehn§, Lindsey L. Glickfeld*, Nobutoshi C. Harata*, Yuqing Cao*, Ege T. Kavalali*¶, Patrick O. Brown§, and Richard W. Tsien*‖

*Department of Molecular and Cellular Physiology, Beckman Center, and §Department of Biochemistry, Center for Clinical Science Research, Stanford University School of Medicine, Stanford, CA 94305-5345

Contributed by Richard W. Tsien, December 24, 2003

At central synapses, P/Q-type Ca^{2+} channels normally provide a critical Ca^{2+} entry pathway for neurotransmission. Nevertheless, we found that nerve terminals lacking α_{1A} ($Ca_V2.1$), the pore-forming subunit of P/Q-type channels, displayed a remarkable preservation of synaptic function. Two consistent physiological changes reflective of synaptic homeostasis were observed in cultured hippocampal neurons derived from α_{1A} (−/−) mice. First, the presynaptic response to an ionophore-mediated Ca^{2+} elevation was 50% greater, indicating an enhanced Ca^{2+} sensitivity of the release machinery. Second, basal miniature excitatory postsynaptic current frequency in α_{1A} (−/−) neurons was increased 2-fold compared with WT neurons and occluded the normal response of presynaptic terminals to cAMP elevation, suggesting that the compensatory mechanism in α_{1A} (−/−) synapses and the modulation of presynaptic function by PKA might share a final common pathway. We used cDNA microarray analysis to identify molecular changes underlying homeostatic regulation in the α_{1A} (−/−) hippocampus. The 40,000 entries in our custom-made array included likely targets of presynaptic homeostasis, along with many other transcripts, allowing a wide-ranging examination of gene expression. The developmental pattern of changes in transcript levels relative to WT was striking; mRNAs at 5 and 11 days postnatal showed little deviation, but clear differences emerged by 22 days. Many of the transcripts that differed significantly in abundance corresponded to known genes that could be incorporated within a logical pattern consistent with the modulation of presynaptic function. Changes in endocytotic proteins, signal transduction kinases, and candidates for Ca^{2+}-sensing molecules were consistent with implications of the direct physiological experiments.

Homeostasis, the basic process by which living systems maintain their functions within an appropriate physiological range, is particularly vital at synapses of the CNS. Synapses regulate their strength with feedback, a mechanism that avoids the extremes of complete quiescence or excessive action potential firing. Synaptic homeostasis must work in conjunction with synaptic plasticity that supports learning and memory. Biological neural networks must balance the need for both singular and global synaptic changes; maintaining the strengths of individual connections is required to encode information in a synaptic network, and controlling the total strength of all inputs is required to maintain output firing within reasonable limits. In principle, the strength of an individual synapse and the global control of all inputs can both be maintained by active feedback. In the absence of such maintenance, the strength of synaptic connections would be subject to "drift" over time. Thus, synaptic homeostasis helps ensure that neurons in the brain continue to function appropriately throughout life.

The awareness of feedback regulation at synapses is growing (1, 2). Some molecular factors support such adjustments (3, 4) and some physiological mechanisms have been proposed, such as changes in postsynaptic receptor composition (5, 6). Work at the neuromuscular junction has uncovered other forms of synaptic homeostasis whereby purely postsynaptic interventions cause alterations in presynaptic function (3, 4, 7, 8). However, no clear picture has emerged of the underlying molecular mechanisms that control presynaptic homeostasis.

We sought to understand the nature of active feedback mechanisms through perturbation experiments, investigating consequences of the genetic removal of the pore-forming α_{1A} subunit of the P/Q-type Ca^{2+} channel. This intervention offered an excellent setting to study synaptic homeostasis. The P/Q-type calcium channel is a presynaptic linchpin, joining the mechanisms regulating presynaptic membrane potential with the biochemical and vesicle trafficking events leading to neurotransmitter secretion. Acute pharmacological blockade of this channel largely attenuates neurotransmission (9). Chronic removal of this normally dominant Ca^{2+} entry pathway does not greatly attenuate transmission; on the contrary, synaptic transmission looks surprisingly intact (10). Manipulations of this kind are more informative perturbations than deletion of an element absolutely required for secretion that leads to general synaptic failure. Genetic deletion of P/Q-type calcium channels is particularly interesting because of the strong involvement of α_{1A} in neurological diseases, arising from autoimmunity (Lambert–Eaton myasthenic syndrome) or genetics (SCA6, FHM, and EA2). The exact mechanism of these disease states is unknown; however, general synaptic failure can be ruled out because the majority of these channel pathologies involve only subtle changes in α_{1A} function. Here we report on the physiological profile and associated molecular mechanisms governing the homeostasis at central nerve terminals after the deletion of the a_{1A} subunit.

Methods

Cell Culture. Hippocampal neurons of 1-day-old knockout and WT mice were prepared in sparse culture according to previous protocols (1) with minor modifications. Cultures were used after 10–14 days *in vitro*.

Dye Loading and Destaining. Presynaptic terminals were labeled by exposure to styryl dye (8 μM FM1-43) during high-K^+ depolarization (modified Tyrode's solution's solution containing 45 mM KCl) or by field stimulation (platinum bath electrodes delivering 30 mA/ms per pulse). Dye was allowed to remain in the extracellular solution for 30 s followed by a constant wash for 15 min (2 ml/min). All staining and washing protocols were performed with modified Tyrode's solution containing 10 μM 6-cyano-7-nitroquinoxaline-2,3-dione to prevent recurrent activity. Fluorescence images were obtained by a cooled, intensified charge-coupled device camera (Stanford Photonics, Palo Alto, CA) during repetitive arc lamp illumination (480 nm) by an optical switch (Solamere Technology Group, Salt Lake City). Images were digitized and processed with

Abbreviations: mEPSC, miniature excitatory postsynaptic current; CAMK, calmodulin-dependent protein kinase.

†E.S.P.-R. and J.L.P. contributed equally to this work.

‡Present address: Department of Cellular and Molecular Physiology, Loyola University Chicago, Maywood, IL 60153-5500.

¶Present address: Center for Basic Neuroscience, University of Texas Southwestern, Dallas, TX 75219.

‖To whom correspondence should be addressed. E-mail: rwtsien@stanford.edu.

Image Lightning and Imaging Workbench (Axon Instruments, Union City, CA) and later analyzed with custom software.

Electrophysiology. Spontaneous miniature excitatory postsynaptic currents (mEPSCs) were recorded by whole-cell patch clamp by using an Axopatch 200B amplifier with CLAMPEX 8.0 software (Axon Instruments). Patch pipettes were pulled from borosilicate glass to a tip diameter corresponding to a resistance of 2–4 MΩ. Internal solution included 135 mM cesium gluconate, 10 mM EGTA, 2 mM $MgCl_2$, 5 mM Mg-ATP, and 10 mM Hepes (pH 7.35). Series resistance and cell capacitance were compensated at the 50–75% level, and the data were filtered at 5 kHz by an eight-pole Bessel filter.

Electron Microscopy. Cultured neurons were fixed with 2% glutaraldehyde in 100 mM cacodylate buffer and washed with 100 mM cacodylate containing 150 mM sucrose. Thereafter, they were processed in a Pelco 3450 microwave oven (Ted Pella, Redding, CA). They were postfixed in 2% osmium tetroxide in 100 mM cacodylate buffer, *en bloc* stained with 5% aqueous uranyl acetate, dehydrated in an ascending ethanol series, and infiltrated in EMbed 812 resin (Electron Microscopy Sciences, Fort Washington, PA). Thin sections (50–70 nm) were cut parallel to the coverslip surface and were poststained with 5% aqueous uranyl acetate and Sato's lead citrate. Sections were examined at 80-kV accelerating voltage by Philips 410. Docked vesicles were defined as the ones with the outer vesicular membrane in direct contact with the active zone. Numbers of vesicles in WT and knockout mice were analyzed in a blind manner.

Expression Analysis. A series of control experiments were carried out to set limits on the variability of the cDNA microarray assay of relevance to determining the statistical significance of changes in mRNA expression detected by the microarrays. A clonal cell line (Jurkat T cells) was split into eight separate flasks and grown in suspended culture. mRNA from each group of cells was isolated separately, processed into cDNA, and prepared for competitive hybridization against a human cDNA microarray array (3,700 spots). The reference standard was cDNA prepared from one of the flasks. As a standard for spot intensity, we excluded any spots whose fluorescence was not >3-fold greater than the immediately surrounding background. Furthermore, as a test for homogeneity across the spot, we compared the intensities of the two fluorescence signals for each individual pixel within the spot and required a correlation coefficient of >0.6 for the spot to be included in the analysis. Looking separately across the eight distinct cDNA microarrays, the resulting histograms of cDNA ratios (of all acceptable spots) were invariably Gaussian distributions, with a peak very close to 1.00 and an average variance of 0.08 (mean standard deviation of 0.29 ± 0.01, mean ± SEM). Array data from age- and gender-matched $\alpha_{1A}-/-$ and WT littermates were compared at different stages of development. Distributions of knockout/WT cDNA ratios derived from 5-, 11-, and 22-day animals had variances of 0.07, 0.05, and 0.22, respectively. The similarity of variance values at 5 and 11 days to those obtained in the control experiments with clonal cells suggested that undetectable differences existed between the expression profiles of 5- and 11-day knockout and WT hippocampi. The sharply increased variance at 22 days indicated a significantly different profile of gene expression between the knockout mice and their WT counterparts.

To quantify accurately changes in the expression of specific genes of 22 postnatal day hippocampus, we performed repeated expression experiments. Hippocampi from eight pairs of 22-day-old, gender-matched α_{1A} knockout and WT siblings were harvested and processed for analysis on cDNA microarrays. To minimize error associated with using a standardized reference, we competitively hybridized α_{1A} knockout and WT expression products directly against one another. The mean spot fluorescence intensity was

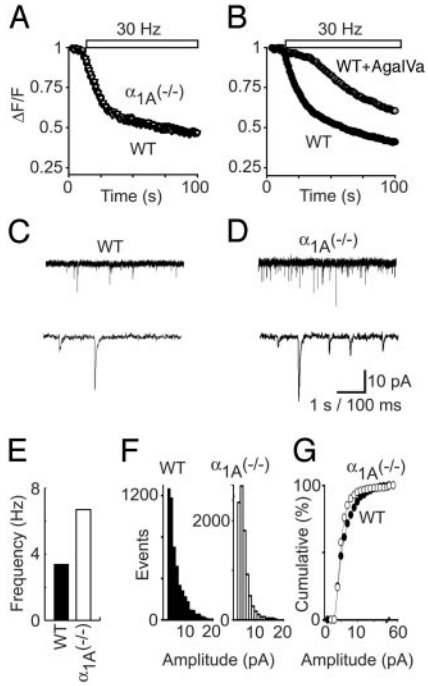

Fig. 1. α_{1A} (−/−) nerve terminals possess a form of presynaptic homeostasis. (*A*) Hippocampal nerve terminals labeled with FM1-43 release the dye during 30-Hz field stimulation. Despite the loss of a critical Ca^{2+} entry pathway, α_{1A} (−/−) terminals release FM1-43 with the same time course as WT terminals. (*B*) Acute blockade of α_{1A} Ca^{2+} channels with ω-Agatoxin IVA severely impairs neurotransmission, illustrating the dependence of WT neurotransmission on the P/Q-type calcium current. (*C* and *D*) Spontaneous mEPSCs recorded from WT and α_{1A} (−/−) hippocampal neurons in culture. (*E*) The average frequency of mEPSCs in α_{1A} (−/−) neurons is approximately twice that of WT terminals (6.7 ± 0.1 and 3.4 ± 0.1 Hz, respectively). (*F* and *G*) The amplitude of mEPSCs from α_{1A} (−/−) hippocampal neurons (5.7 ± 0.04 pA) was slightly less than the amplitude of mEPSCs from WT neurons (6.3 ± 0.04 pA, $P < 0.001$).

1,800 arbitrary fluorescent units (A.U.) in a 10-bit scale; the mean fluorescence intensity of the cDNA array background was 151 ± 0.3 A.U. We excluded all spots from analysis whose fluorescence intensity divided by the intensity of the background immediately surrounding the spot did not exceed 3. Spots with <10 analyzable pixels were excluded. Spots with >10 analyzable pixels were further evaluated for homogeneity; the spot was excluded if the regression correlation of the two-channel fluorescence intensity of all pixels within the spot did not exceed 0.6. Once cDNA spots had met all inclusion criteria, we calculated the average, standard deviation, standard error of the mean (σ), and *t* statistic for each gene on the array. Spots from certain genes were usable from all eight arrays, whereas other genes had less than eight usable data points for statistical analysis. The number of acceptable spots for each gene is indicated in the legends to Figs. 3–5 and was appropriately reflected in all statistics.

Results

We compared the properties of synaptic vesicle turnover at $\alpha_{1A}-/-$ and WT synapses from hippocampal neurons. Despite the chronic absence of P/Q-type Ca^{2+} channels, neurotransmitter release was robust in $\alpha_{1A}-/-$ synapses. The dynamics of activity-dependent secretory function at single nerve terminals were explored by monitoring activity-dependent uptake and release of FM1-43 (Fig. 1 *A* and *B*). This lipid dye fluoresces brightly in synaptic terminals when taken up and trapped by synaptic vesicles undergoing exo/endocytotic cycling (11). Presynaptic vesicular turnover was monitored as the loss of FM dye fluorescence during field stimulation

at 30 Hz. Remarkably, $\alpha_{1A}-/-$ terminals released FM1-43 with a time course virtually identical with WT terminals (Fig. *1A*). In sharp contrast, acutely inhibiting P/Q-type Ca^{2+} channels with the specific blocker ω-Aga-IVA caused a great reduction in the rate of FM1-43 loss (Fig. 1*B*), consistent with the predominance of P/Q-type Ca^{2+} channels in WT neurotransmission (9). The equivalence of vesicular turnover kinetics at $\alpha_{1A}-/-$ and WT synapses suggested that deficits in excitation-secretion coupling were perceived and corrected for in hippocampal synapses lacking the α_{1A} subunit.

To learn more about possible mechanisms of compensation at single synaptic sites, we carried out whole-cell recordings of spontaneous miniature excitatory postsynaptic currents (mEPSCs). Fig. 1 *C* and *D* compares mEPSC recordings from WT (Fig. 1*C*) and $\alpha_{1A}-/-$ pyramidal neurons (Fig. 1*D*). The frequency of mEPSCs was increased by 2-fold (3.4 ± 0.1 to 6.7 ± 0.1 Hz), a consistent finding in numerous recordings (Fig. 1*E*). Several studies have suggested a unifying relationship between synaptic strength, spontaneous release, and the state of release machinery molecules. The increase in mini frequency after a chronic presynaptic lesion pointed to a potential locus for homeostatic regulation of synaptic terminals. Certain perturbations, such as cAMP-stimulating drugs, tonic stimulation, and genetic knockouts of vesicle proteins, have been shown to alter the spontaneous release rate by altering the function of molecules that initiate or regulate the release of presynaptic vesicles. Despite these findings, we considered the possibility that changes in the number of postsynaptic glutamate receptors led to the increase in observed spontaneous release events (Fig. 1*F*). However, the amplitude of mEPSCs originating from $\alpha_{1A}-/-$ nerve terminals (5.7 ± 0.04 pA) was, if anything, slightly smaller than those from WT (6.3 ± 0.04 pA, $P < 0.001$). Thus, alterations in postsynaptic receptors are not a likely explanation of the enhanced mEPSC frequency; rather, the evidence points consistently to a presynaptic mechanism.

The increased mini frequency could be attributed to a greater abundance of functional nerve terminals or an increase in the rate of spontaneous release from individual terminals. For example, synaptic perturbations at the *Drosophila* neuromuscular junction are known to change the number of functional synapses without altering the distribution of mEPSC amplitudes. We looked for changes in synapse abundance in our hippocampal cultures by immunostaining for the presynaptic marker synapsin 1 (Fig. 2*A*). The $\alpha_{1A}-/-$ hippocampal cultures were no different from WT in either the number or spatial distribution of synaptic terminals. To assess the abundance of synapses that were presynaptically active, we counted the number of nerve terminals that became labeled with FM-143 during the course of prolonged stimulation (Fig. 2*B*). Again, $\alpha_{1A}-/-$ and WT hippocampal cultures were identical in the number and area of FM1-43 puncta. Because no increase was found in either the total number of synaptic terminals or the abundance of active terminals, we turned next to a detailed comparison at the ultrastructural level.

Electron microscopy failed to reveal any qualitative morphological features that distinguished $\alpha_{1A}-/-$ terminals from their WT counterparts (Fig. 2*C*). On further analysis, no significant differences ($P > 0.05$) were found in the size of the total presynaptic vesicle pool (Fig. 2*D*). Small but significant quantitative differences were observed in two respects. The number of docked vesicles per section was greater in the $\alpha_{1A}-/-$ terminals, as determined in double-blind comparisons, increasing from 3.3 ± 0.1 vesicles in WT to 4.2 ± 0.2 vesicles in knockout mice ($P < 0.01$) (Fig. 2*E*). Likewise, the active recycling pool of synaptic vesicles was slightly larger in $\alpha_{1A}-/-$ boutons than in WT (Fig. 2*F*), shown by FM1-43 labeling of the total recycling pool (12). Because no differences were found in vesicle size or morphology with electron microscopy, this finding suggested that the absence of P/Q-type channels increased the proportion of functional synaptic vesicles without increasing the total number of vesicles per terminal.

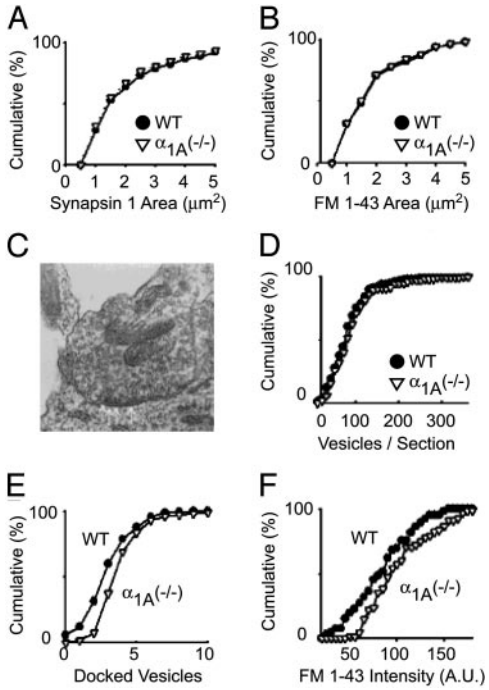

Fig. 2. α_{1A} (−/−) neurons have the same number of synapses but their presynaptic terminals have detectable ultrastructural differences. (*A*) The total number of synapses and (*B*) the number of functional synapses formed by α_{1A} (−/−) hippocampal neurons is identical with WT neurons. (*C*) The ultrastructure of α_{1A} (−/−) synapses is qualitatively the same as WT synapses. (*D*) The number of synaptic vesicles in α_{1A} (−/−) presynaptic terminals is indistinguishable from WT terminals. (*E*) Double-blind comparison of the number of docked vesicles per EM section. α_{1A} (−/−) synapses have more docked vesicles per section than WT terminals (WT, 3.3 ± 0.1; α_{1A} (−/−), 4.2 ± 0.2 docked vesicles per section; $P < 0.01$). (*F*) Presynaptic terminals maximally labeled with FM1-43 to determine the size of the active pool of synaptic vesicles. α_{1A} (−/−) presynaptic terminals have a larger active pool of synaptic vesicles than WT terminals ($P < 0.01$).

We set out to identify molecular alterations underlying the homeostasis in nerve terminals lacking P/Q-type Ca^{2+} channels. Encouraged by reports of specific genes that support other forms of synaptic stability (13), we measured changes in cellular mRNA expression profiles by using cDNA microarrays. We constructed a 24,400-spot *Mus musculus* cDNA microarray consisting of 18,000 random expressed sequence tags plus several thousand genes identified as important in neuronal development, synaptic transmission, or signal transduction. Knowing that compensatory changes in gene expression occur gradually over time after perturbation of synaptic transmission (2), we first investigated multiple time points. Messenger RNA was isolated and prepared from hippocampi of age- and gender-matched $\alpha_{1A}-/-$ animals and their WT siblings to minimize extraneous biological variation. cDNA was polymerized from the mRNA template in the presence of fluorescently labeled nucleotides and competitively hybridized on our cDNA microarray. The resulting fluorescence intensities were measured by a laser-scanning array-imaging device (Genepix, Axon Instruments, Union City, CA) to yield ratios of $\alpha_{1A}-/-$ to WT expression for each microarray spot.

The CNS expression of α_{1A} and the behavioral deficits in α_{1A} knockout mice occur primarily after the second postnatal week (10). Fig. 3*A* displays the ratio of $\alpha_{1A}-/-$ gene expression over WT at 5, 11, and 22 postnatal days. Columns in the gene bar represent individual genes, whereas the rows represent 5-, 11-, and 22-day-old $\alpha_{1A}-/-$ vs. WT samples. Red indicates that the expression of the gene in that column was significantly up-regulated, whereas green indicates that it was down-regulated (14). Significant differences in

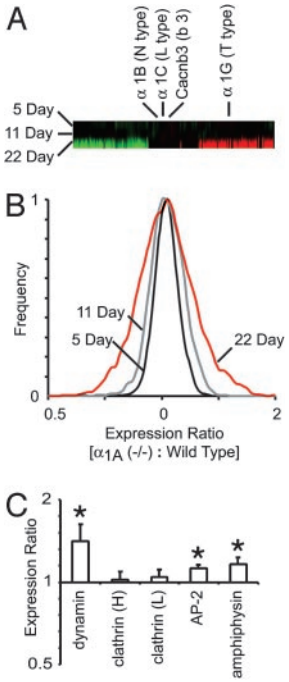

Fig. 3. mRNA from 5-, 11-, and 22-day α_{1A} (−/−) and WT hippocampus were evaluated by direct, competitive hybridization onto custom-made *M. musculus* cDNA microarrays. (*A*) α_{1A} (−/−) neurons showed few detectable changes in their cellular mRNA expression profile before the third postnatal week. Red indicates that the expression of the gene in that column was significantly up-regulated, and green indicates that it was down-regulated. A substantial number of genes were up- and down-regulated in the α_{1A} (−/−) hippocampus by postnatal day 22; however, the two high-voltage-activated Ca^{2+} channel subunits (α_{1B} and α_{1C}) that could have potentially replaced P/Q-type calcium currents showed no change in their mRNA expression levels at 5, 11, or 22 days postnatal. (*B*) The variance in the mRNA expression profile of 5- and 11-day α_{1A} (−/−) vs. WT hippocampus (0.07 and 0.05) is similar to the detection variance of the cDNA microarray (0.08; see *Methods*). The variance of 22-day α_{1A} (−/−) vs. WT hippocampus experiments (0.22) indicates that appreciable up- and down-regulation of genes had occurred by this day. (*C*) Hippocampi from eight pairs of 22-day-old, gender-matched α_{1A} knockout and WT siblings were analyzed by 40,000-spot cDNA microarrays. Where the mRNA from the α_{1A} (−/−) sample differed from the control, the significance level was shown by *, $P < 0.05$, and **, $P < 0.01$. Of major endocytotic proteins, the expression of dynamin was up-regulated significantly (1.4 ± 0.12, $n = 8$, $P < 0.05$), whereas the expression of the heavy and light chains of clathrin remained unchanged. AP-2 and amphiphysin, two molecules important in the endocytotic protein complex, were up-regulated as well (1.13 ± 0.03, $n = 8$, $P < 0.05$; 1.16 ± 0.07, $n = 8$, $P < 0.05$, respectively).

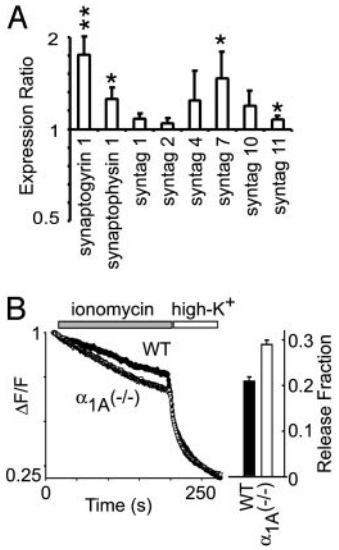

Fig. 4. The vesicle release machinery of α_{1A} (−/−) presynaptic terminals is more sensitive to Ca^{2+} than WT terminals. (*A*) The mRNA levels of molecules known to regulate the Ca^{2+} sensitivity of the presynaptic release machinery. Synaptogyrin 1 and synaptophysin 1 were significantly up-regulated (1.8 ± 0.2, $n = 6$, $P < 0.01$; 1.3 ± 0.1, $n = 8$, $P < 0.05$, respectively). Synaptotagmin 7, a Ca^{2+} sensor-interacting molecule was significantly up-regulated (1.6 ± 0.3, $n = 6$, $P < 0.05$). Synaptotagmins 1 and 2, two Ca^{2+}-sensing molecules involved in the regulation of fast Ca^{2+}-dependent presynaptic release, did not change. (*B*) The Ca^{2+} ionophore, ionomycin, releases synaptic vesicles from presynaptic terminals independent of voltage-gated Ca^{2+} channels. When challenged by ionomycin, α_{1A} (−/−) presynaptic terminals released synaptic vesicles ≈50% faster than WT terminals.

transcription were found in $\alpha_{1A}-/-$ and WT hippocampus at 22 days, but not at 5 and 11 days postnatal (Fig. 3*B*). This finding was consistent with behavioral and molecular data showing that neurotransmission does not become reliant on α_{1A} Ca^{2+} channels until after the early postnatal period (10). We were able to assess whether altered expression of Ca^{2+} channels rescued the presynaptic release mechanism (Fig. 3*A*). The most obvious candidate is the N-type Ca^{2+} channel α_1 subunit, α_{1B} ($Ca_v2.2$), which predominates hippocampal synaptic transmission in $\alpha_{1A}-/-$ slices (10). However, we found no significant change in the expression of α_{1B}, nor in the L-type α_1 subunit, α_{1C} ($Ca_v1.2$), another high-voltage-activated Ca^{2+} channel family member. We also examined expression of α_{1G} ($Ca_v3.1$), a representative of the third subfamily of Ca^{2+} channels whose pore-forming subunits support low-voltage-activating, transient T-type Ca^{2+} currents. α_{1G} showed significantly increased expression (1.4-fold) at the 22-postnatal-day time point. T-type currents are known to influence repetitive neuronal firing and epileptiform activity, so it is possible that the increased expression of α_{1G} contributed to enhanced propensity for seizures in the knockout mice. However, none of the findings with regard to Ca^{2+} channel expression provided a plausible explanation for the synaptic homeostasis we observed. Likewise, expression analysis of α-amino-3-hydroxy-5-methyl-4-isoxazolepropionic acid receptor subtypes showed no significant alteration in the mRNA levels, a result not surprising in view of the lack of major change in mEPSC amplitude in $\alpha_{1A}-/-$ nerve terminals.

To characterize the gene expression of 22-day-old animals in greater detail, we expanded the cDNA array with 18,000 additional spots and performed eight parallel experiments directly comparing mRNA expression in $\alpha_{1A}-/-$ hippocampi with that in hippocampi from age- and gender-matched WT siblings. A total of 30,830 hybridized spots fulfilled criteria to be considered adequate for analysis (*Methods*). Of the ≈80% unique genes, a total of 927 spots showed a statistically significant increase in the ratio of $\alpha_{1A}-/-$ to WT mRNA (mean ≥ 1.25, $\sigma < 0.15$); a total of 474 spots showed a statistically significant decrease (mean < 0.8, $\sigma < 0.15$).

The increase in size of the total recycling pool, monitored by uptake of dye fluorescence, prompted us to examine the level of mRNA expression of key molecules in endocytotic pathways (Fig. 3*C*). One significantly up-regulated molecule was dynamin, a small GTPase essential in the formation of coated vesicles and suspected to be central in kiss-and-run modes of endocytosis. Expression of the light and heavy chains of clathrin remained unchanged, whereas the accessory molecules, AP-2 and amphiphysin, were slightly up-regulated.

Altering the Ca^{2+} sensitivity of the release machinery would be an effective way to compensate for the loss of spatially optimal Ca^{2+} entry by P/Q-type Ca^{2+} channels. This would increase the participation of other types of Ca^{2+} channels perhaps more distant from Ca^{2+} sensors, as suggested by experiments on neuromuscular transmission (15). Accordingly, we evaluated changes in the expression of molecules thought to support Ca^{2+}-sensitive signaling in presynaptic terminals (Fig. 4*A*). Significant up-regulation was found in the measured mRNA levels of synaptogyrin 1 and synaptophysin

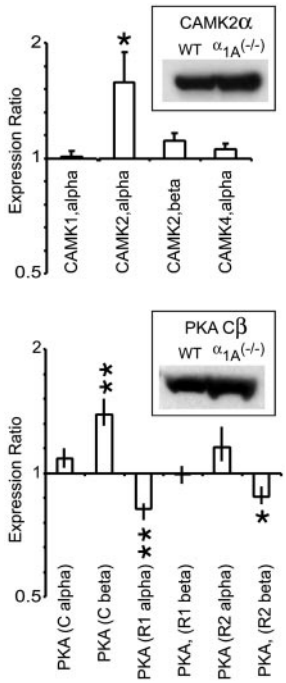

Fig. 5. The mRNA profiles of Ca^{2+}/calmodulin-dependent protein kinases and cAMP-dependent protein kinases show significant alterations in the α_{1A} (−/−) hippocampus. The mRNA of two important synaptic kinases, CAMK2α and PKA(Cβ), were significantly up-regulated in the 22-postnatal-day α_{1A} (−/−) hippocampus (1.6 ± 0.27, $n = 3$, $P < 0.05$; 1.4 ± 0.13, $n = 8$, $P < 0.01$, respectively). These kinases are widely studied for their powerful modulatory effects on synaptic transmission. Also of interest was the down-regulation of two regulatory PKA subunits, R1α and R2β (0.82 ± 0.03, $n = 8$, $P < 0.01$; 0.87 ± 0.05, $n = 5$, $P < 0.01$, respectively). (*Insets*) Western blots of CAMK2 and PKA isoforms confirmed that increased mRNA led to increased protein levels in α_{1A} (−/−) hippocampus.

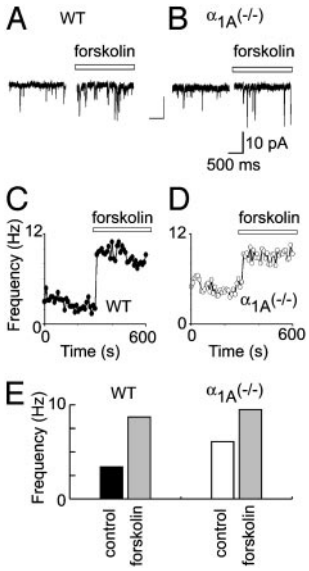

Fig. 6. The PKA-signaling pathway is an important component of synaptic homeostasis in α_{1A} (−/−) presynaptic terminals. (*A*) The application of forskolin dramatically increased the mEPSC frequency of WT terminals (3.4 ± 0.1 to 8.7 ± 0.1 Hz). (*B*) An identical application of forskolin to α_{1A} (−/−) synapses increased mEPSC frequency from 6.1 ± 0.1 to 9.5 ± 0.1. (*C* and *D*) The mEPSC frequency of WT and α_{1A} (−/−) synapses was elevated to similar levels by increasing cAMP signaling with forskolin (to 8.7 ± 0.1 and 9.5 ± 0.1 Hz, respectively). (*E*) Pooled data indicated that the increase in mEPSC frequency in α_{1A} (−/−) nerve terminals was fully occluded by PKA-induced presynaptic modulation ($P > 0.6$).

1, two molecules that serve overlapping but essential functions in several Ca^{2+}-dependent forms of synaptic plasticity: paired-pulse facilitation, posttetanic potentiation, and long-term potentiation (16, 17). We also looked for specific patterns of expression change in the synaptotagmins, an important family of presynaptic proteins for fast excitation-secretion coupling and Ca^{2+}-dependent endocytosis. Of the ten synaptotagmins represented on our cDNA microarray, only synaptotagmin 7 showed a significant difference in mRNA expression, an ≈1.6-fold elevation in α_{1A}−/− relative to WT. We found this increase rather intriguing because of new evidence suggesting that synaptotagmin 7, a plasma membrane-bound Ca^{2+}-sensing molecule, acts in conjunction with the putative exocytotic Ca^{2+} sensors synaptotagmin 1 and 2 to regulate endocytotic pathways (18).

To test directly for a change in the Ca^{2+} sensitivity of presynaptic release machinery, we stimulated vesicular turnover by application of ionomycin, a Ca^{2+} ionophore that bypasses the need for voltage-gated Ca^{2+} channels (19, 20). Application of ionomycin to FM1-43-loaded presynaptic nerve terminals led to an immediate loss of fluorescence due to Ca^{2+}-induced vesicle fusion (Fig. 4*B*). Vesicle release from α_{1A}−/− nerve terminals was significantly augmented relative to control. In multiple experiments, the release of fluorescent dye from α_{1A}−/− averaged ≈50% greater than the response in WT terminals. This directly demonstrated that the deletion of the α_{1A} subunit resulted in presynaptic release machinery with a greater sensitivity to Ca^{2+}.

Ca^{2+}/calmodulin-dependent protein kinases are foremost among the many signal transduction pathways that link electrical activity to long-term modification of neuronal properties. Of the five calmodulin-dependent protein kinase (CAMK) isoforms available on the cDNA microarray, only CAMKIIα showed significant modification in α_{1A}−/− hippocampus, a 1.5-fold increase in mRNA expression (Fig. 5). Western blot analysis confirmed our gene expression data in showing that the CAMKII α expression was increased at the level of protein (Fig. 5 *Inset*) as well as mRNA. Increases in the α/β ratio within the multimeric CAMKII complex are thought to decrease overall Ca^{2+}/calmodulin sensitivity of the holoenzyme. Thus, the observed changes would desensitize CAMKII, contrary to what would be expected for a homeostatic synaptic mechanism.

cAMP-dependent protein kinase (PKA), a well known regulator of hippocampal synaptic transmission, can be recruited during neuronal activity after increases in cAMP either through the action of neuromodulators on G protein-coupled receptors or through activation of Ca^{2+}-dependent adenylyl cyclases. The PKA protein complex, consisting of two regulatory subunits and two catalytic subunits (R_2C_2), becomes activated when binding of cAMP to C subunits triggers their release from the tetrameric complex and liberation of their catalytic sites. Alterations in cellular levels of various R subunits (RIα, RIβ, RIIα, and RIIβ) and C subunits (Cα and Cβ) are thought to tune the sensitivity and location of PKA activity. Among the six possible components of PKA, only the Cβ and RIα subunits showed significant changes in mRNA expression, Cβ increasing and RIα decreasing in the α_{1A}−/− hippocampus (Fig. 5*B*). This finding was also confirmed by Western blot analysis, which supported a clear increase in Cβ at the level of protein. Because Cβ is more cAMP-sensitive than Cα, this change would tend to increase PKA activity, in line with expectations if PKA were involved in the synaptic compensation (21–24).

The altered expression of PKA subunits in the α_{1A}−/− hippocampus raised the possibility that PKA signaling might contribute to homeostatic control of presynaptic function. This possibility was explored by testing the effects of forskolin, a direct stimulator of adenylate cyclase. At WT synapses, forskolin caused a sharp increase in the frequency of mEPSCs, from 3.3 ± 1.7 to 8.5 ± 1.5 Hz ($P < 0.01$) (Fig. 6*A*), without an alteration in mEPSC amplitude

(data not shown), consistent with published studies. The critical experiment was to examine the effect of raising cAMP in the $\alpha_{1A}-/-$ presynaptic terminals. If the PKA modulation and synaptic compensation acted by completely independent mechanisms, one would expect additive or even multiplicative responses in mEPSC rate. On the contrary, we found that the forskolin-induced increase in mEPSC frequency in nerve terminals lacking α_{1A} consistently reached a maximum level (9.6 ± 0.3 Hz, mean ± SEM; $n = 4$) not significantly greater than in WT (8.5 ± 0.1 Hz, mean ± SEM; $n = 5$) ($P > 0.6$). Thus, the mechanism responsible for mEPSC frequency increase in α_{1A} $(-/-)$ nerve terminals occluded the PKA-induced presynaptic modulation, indicating convergence onto a similar molecular mechanism.

Discussion

The influence of synaptic homeostasis is evident at synapses lacking the pore-forming subunit of the P/Q-type Ca^{2+} channel. The strength of neurotransmission is remarkably well preserved in the $\alpha_{1A}-/-$ synapse, a striking result because P/Q-type channels are critical for WT transmission and are more efficient in supporting excitation-secretion coupling than N- or R-type channels (15, 25). The preservation of function at the $\alpha_{1A}-/-$ synapse exemplifies a kind of presynaptic homeostasis that is fundamental to CNS transmission, yet poorly understood. Our initial observation that basal mini frequency in $\alpha_{1A}-/-$ neurons was twice as high as in WT neurons provides clear evidence for the existence of a powerful compensatory mechanism operating to augment remaining Ca^{2+} channels.

The molecular mechanisms governing synaptic transmission at central synapses are complicated and incompletely understood; therefore, understanding the mechanisms controlling synaptic homeostasis has been challenging. By applying a wide range of experimental approaches, we were able to exclude many possible compensatory changes, such as abundance of nerve terminals, nerve terminal morphology, vesicle pool size, or the kinetics of vesicular retrieval. Two consistent physiological findings narrowed our search for molecular mechanisms. First, the presynaptic machinery of nerve terminals lacking α_{1A} subunits were more sensitive to Ca^{2+} than their WT counterparts, demonstrated by ionomycin, a Ca^{2+} stimulus that bypassed membrane depolarization and voltage-gated Ca^{2+} channels. The presynaptic response to a generalized Ca^{2+} elevation was 50% greater at P/Q-deficient synapses, indicating directly that the Ca^{2+} sensitivity of the release machinery had been significantly enhanced. Second, synapses lacking P/Q-type channels had an increase in their basal mini frequency (see also ref. 27). We further discovered that the basal increase in $\alpha_{1A}(-/-)$ spontaneous release occluded the normal response of presynaptic terminals to elevation of cAMP, a manipulation well known to increase the spontaneous rate of release at these terminals. This finding suggested that the compensatory mechanism in $\alpha_{1A}(-/-)$ synapses and the modulation of presynaptic function by PKA shared a final common pathway. Our results support previous experiments that suggest that PKA augments presynaptic transmitter release by working downstream of Ca^{2+} influx, a modulation that acts directly on the molecular apparatus linking Ca^{2+} concentration to vesicle fusion (21, 26).

To identify molecular changes underlying homeostatic regulation, we combined the aforementioned approaches with state-of-the-art cDNA microarrays. This report uses previously unused gene microarray technology to study how synaptic strength is dynamically regulated. The 40,000 entries in our custom-made array included likely targets of presynaptic homeostasis, along with a multitude of other transcripts, to gain a broad and relatively unbiased profile of gene expression. The developmental pattern of changes in transcript levels and altered protein synthesis was striking (see also ref. 28). We found a gene expression profile in knockout animals that displayed very few differences relative to WT at 5 and 11 days postnatal, but showed significant changes by 22 days postnatal. This gene expression profile is precisely the temporal profile one would expect for events dependent on α_{1A}, a channel that only becomes functionally important after 11 postnatal days.

The advantages of large-scale mRNA transcription analysis were immediately evident. Transcripts of many candidate genes that might be expected *a priori* to differ in $\alpha_{1A}(-/-)$ and WT hippocampus—the N-type Ca^{2+} channel, cAMP-response element-binding protein and their expression targets, and synaptotagmin I—were not significantly altered. On the other hand, the arrays uncovered other candidates that might well have been overlooked: synaptogyrin I and synaptophysin I, molecules thought to play overlapping roles in Ca^{2+}-dependent presynaptic modulation, and synaptotagmin VII, a binding partner of the fast exocytotic Ca^{2+} sensors (18). Even at 22 days postnatal, only a minor fraction of transcripts differed significantly in abundance, perhaps befitting homeostatic changes with a relatively confined cellular locus. Those mRNAs that did differ could be incorporated within a logical pattern consistent with the modulation of presynaptic function. For example, significant alterations in levels of kinase subunits were found and may potentially contribute to the modulation. The endocytotic protein, dynamin, plays a central role in the vesicle cycle of small central terminals. The synaptotagmin family members are Ca^{2+}-sensing proteins known to regulate the Ca^{2+}-dependent properties of neurotransmitter release. Further work is needed to evaluate the roles of all the molecules involved in synaptic transmission and modulation, but it is clear that homeostatic mechanisms include specific increases in the roles of endocytotic, signal transduction kinases, and Ca^{2+}-sensing molecules. The advent of cDNA microarrays enables a kind of experimental approach, exemplified by this study: wide-ranging examination of changes in patterns of gene expression, generation of hypotheses, all feeding back to basic physiological experiments to test the hypotheses directly.

1. Liu, G. & Tsien, R. W. (1995) *Nature* **375,** 404–408.
2. Turrigiano, G. G., Leslie, K. R., Desai, N. S., Rutherford, L. C. & Nelson, S. B. (1998) *Nature* **391,** 892–896.
3. Davis, G. W. & Bezprozvanny, I. (2001) *Annu. Rev. Physiol.* **63,** 847–869.
4. Paradis, S., Sweeney, S. T. & Davis, G. W. (2001) *Neuron* **30,** 737–749.
5. Golowasch, J., Abbott, L. F. & Marder, E. (1999) *J. Neurosci.* **19,** RC33.
6. Turrigiano, G., LeMasson, G. & Marder, E. (1995) *J. Neurosci.* **15,** 3640–3652.
7. Petersen, S. A., Fetter, R. D., Noordermeer, J. N., Goodman, C. S. & DiAntonio, A. (1997) *Neuron* **19,** 1237–1248.
8. Sandrock, A. W., Jr., Dryer, S. E., Rosen, K. M., Gozani, S. N., Kramer, R., Theill, L. E. & Fischbach, G. D. (1997) *Science* **276,** 599–603.
9. Wheeler, D. B., Randall, A., Sather, W. A. & Tsien, R. W. (1995) *Prog. Brain Res.* **105,** 65–78.
10. Jun, K.-S., Piedras-Rentería, E. S., Smith, S. M., Wheeler, D. B., Lee, S. B., Lee, T. G., Chin, H., Adams, M. E., Scheller, R. H., Tsien, R. W. & Shin, H.-S. (1999) *Proc. Natl. Acad. Sci. USA* **96,** 15245–15250.
11. Cochilla, A. J., Angleson, J. K. & Betz, W. J. (1999) *Annu. Rev. Neurosci.* **22,** 1–10.
12. Harata, N., Pyle, J. L., Aravanis, A. M., Mozhayeva, M., Kavalali, E. T. & Tsien, R. W. (2001) *Trends Neurosci.* **24,** 637–643.
13. Thiagarajan, T. C., Piedras-Renteria, E. S. & Tsien, R. W. (2002) *Neuron* **36,** 1103–1114.
14. Eisen, M. B., Spellman, P. T., Brown, P. O. & Botstein, D. (1998) *Proc. Natl. Acad. Sci. USA* **95,** 14863–14868.
15. Urbano, F. J., P.-R. E., Jun, K., Shin, H. S., Uchitel, O. D. & Tsien, R. W. (2003) *Proc. Natl. Acad. Sci. USA* **100,** 3491–3496.
16. Janz, R., Sudhof, T. C., Hammer, R. E., Unni, V., Siegelbaum, S. A. & Bolshakov, V. Y. (1999) *Neuron* **24,** 687–700.
17. Sugita, S., Janz, R. & Sudhof, T. C. (1999) *J. Biol. Chem.* **274,** 18893–18901.
18. Sugita, S., Han, W., Butz, S., Liu, X., Fernandez-Chacon, R., Lao, Y. & Sudhof, T. C. (2001) *Neuron* **30,** 459–473.
19. Augustin, I., Rosenmund, C., Sudhof, T. C. & Brose, N. (1999) *Nature* **400,** 457–461.
20. Fernandez-Chacon, R., Konigstorfer, A., Gerber, S. H., Garcia, J., Matos, M. F., Stevens, C. F., Brose, N., Rizo, J., Rosenmund, C. & Sudhof, T. C. (2001) *Nature* **410,** 41–49.
21. Sakaba, T. & Neher, E. (2001) *Proc. Natl. Acad. Sci. USA* **98,** 331–336.
22. Mellor, J., Nicoll, R. A. & Schmitz, D. (2002) *Science* **295,** 143–147.
23. Kudoh, S. N., Nagai, R., Kiyosue, K. & Taguchi, T. (2001) *Brain Res.* **915,** 79–87.
24. Blackmer, T., Larsen, E. C., Takahashi, M., Martin, T. F., Alford, S. & Hamm, H. E. (2001) *Science* **292,** 293–297.
25. Regehr, W. G. & Mintz, I. M. (1994) *Neuron* **12,** 605–613.
26. Trudeau, L. E., Fang, Y. & Haydon, P. G. (1998) *Proc. Natl. Acad. Sci. USA* **95,** 7163–7168.
27. Plomp, J. J., Vergouwe, M. N., Van den Maagdenberg, A. M., Ferrari, M. D., Frants, R. R. & Molenaar, P. C. (2000) *Brain* **123,** 463–471.
28. Dabrowski, M., Aerts, S., Van Hummelen, P., Craessaerts, K., De Moor, B., Annaert, W., Moreau, Y. & De Strooper, B. (2003) *J. Neurochem.* **85,** 1279–1288.